applied sciences

MDPI

Article

Design and Development of an Efficiently Harvesting Buoy-Type Wave Energy Converter

Ganesh Korwar [1], Timotei István Erdei [2], Nitin Satpute [3,*], Atul P Kulkarni [1] and Attila Szántó [4,*]

[1] Department of Mechanical Engineering, Vishwakarma Institute of Technology, Pune 411048, Maharashtra, India; ganesh.korwar@vit.edu (G.K.); atul.kulkarni@viit.ac.in (A.P.K.)
[2] Department of Vehicles Engineering, University of Debrecen, Ótemető Str. 2-4, H-4028 Debrecen, Hungary; timoteierdei@eng.unideb.hu
[3] Department of Mechanical Engineering, Vishwakarma University, Pune 411048, Maharashtra, India
[4] Department of Basic Technical Studies, Faculty of Engineering, University of Debrecen, Ótemető Str. 2-4, H-4028 Debrecen, Hungary
* Correspondence: nitinsatpute123@gmail.com (N.S.); szanto.attila@eng.unideb.hu (A.S.)

Abstract

This paper presents an innovative approach to efficiently harvesting energy from ocean waves through a buoy-type Wave Energy Converter (WEC). The proposed methodology integrates a buoy, a Mechanical Motion Rectifier (MMR), a Motion Rectifier (MR), an Energy Storage Element (ESE), and an electric generator. A MATLAB-2023 model has been employed to assess the electrical power generated under varying wave heights and frequencies. Experimental data and numerical simulations reveal that the prototype Wave Energy Harvester (WEH) achieved a peak voltage of 6.7 V, peak power of 3.6 W, and an average power output of 8.5 mW, with an overall efficiency of 47.2% for the device's actual size. Additionally, a theoretical analysis has been conducted to investigate the impact of incorporating additional buoys on the electrical power output.

Keywords: numerical simulation; MMR; MR; ESE; energy harvesting

Academic Editors: Atsushi Mase and José A. Orosa García

Received: 20 August 2025
Revised: 1 October 2025
Accepted: 16 October 2025
Published: 18 October 2025

Citation: Korwar, G.; Erdei, T.I.; Satpute, N.; Kulkarni, A.P.; Szántó, A. Design and Development of an Efficiently Harvesting Buoy-Type Wave Energy Converter. *Appl. Sci.* **2025**, *15*, 11185. https://doi.org/10.3390/app152011185

1. Introduction

Energy harvesting involves capturing and accumulating energy when it is readily available and converting it into usable electric energy. This process is crucial for low voltage and low power applications in various markets such as consumer devices, medical equipment, transportation, industrial control, and military applications. In today's world, major issues like the energy crisis, global warming, and pollution significantly impact humanity. With non-renewable sources on the brink of exhaustion, there is an urgent need for new methods of energy generation. Extensive research is being conducted on energy generation from renewable sources including solar, wind, and sea tides. Renewable energy resources are essential for pollution-free power generation.

Ocean wave power holds great potential, as it can be harnessed for massive electrical power generation. Utilizing ocean wave energy for electric power generation offers several advantages, including economical and year-round availability, the high energy content in deep water waves, and better power density. Waves in deep water have abundant energy, with wave heights ranging from 1m to 10 m. Wave energy is more consistent and predictable than other alternate energy sources, with the highest energy density among renewable sources. Energy harvesting structures for wave energy harvesting can be smaller, less invasive, and more powerful than other renewable sources, including wind and

tide. Ocean wave energy can be utilized for electricity generation using various methods, such as oscillating water columns, oscillating bodies, and overtopping types of devices. Oscillating water columns with the axial flow self-rectifying type of air turbines ensure operational efficiency of up to 57%, and exhibit power density ranging from 13 W/kg to 95.27 W/kg, with fluctuations in sea wave velocity affecting the peak and average power output of these devices [1,2]. Innovative design features in the Oscillating Water Column wave energy harvesters, which use self-pitch-controlled guide vanes, ensure significant improvements in electric power [3–5] investigated the application of different types of turbines including guided vanes, pitch controlled blades, guided vanes, and fixed vanes to wave energy harvesting in areas where the waves have varying and irregular heights. The use of stagnant and stored water in dielectric elastomer generators results in reduced electricity generation capacity [6,7]. Different types of WEC, such as linear sliding wave energy converters (LS-WEC) and rotational WEC, have been proposed to utilize ocean wave energy more effectively [8]. Bou-Mosleh et al. [9] developed and tested a new wave energy converter along the Lebanese coast. This mechanical device comprises a buoy, a rotating pulley, a shaft, antifriction bearings, unidirectional clutch bearings, a spring, a rotating inertial element, and a rotary electric generator. The system could generate a power output of 0.36 W, with an efficiency of approximately 10%. Zanuttigh et al. [10] designed a near-shore floating wave energy converter to harvest energy and avoid sand erosion with negligible environmental and economic construction. The authors conducted experiments on the device at different scales in a custom-made water wave tank at Aalborg University, observing wave transmission, reflection, device interaction, and efficiency under various wave parameters. Abdul Akib et al. [11] conducted a thorough analysis of the WEC comprising the floaters that oscillate in response to passing ocean waves, enabling the translator to oscillate within the stator field and convert the ocean wave power into electrical energy. To enhance the accuracy of the WEC, authors developed a theoretical model of the WEC in MATLAB–Simulink.

Velichkova et al. [12] proposed the design of an integrated system for a wave energy harvester that effectively harnesses kinetic energy in various bodies of water via a combination of a hydraulic turbine with oscillating blades and an air turbine. WEC devices working with piezoelectric generation create strain in a flexible structure through the force of wave motion [13–16]. These devices make use of costly piezoelectric elements and have a power density limit of 30 W/m^2, despite their potential for significant energy generation. Na et al. [17] developed a prototype piezoelectric energy harvester that captures energy from constant wave motion. The technology utilizes the piezoelectric effect in crystals to generate voltage when stressed. The harvester harnesses the impact force of a percussion bar on a bimorph piezoelectric element, yielding an average current of 0.071 mA and a voltage of 2.42 V with an average power of 0.173 mW. Xie et al. [18] developed an ocean WEC to utilize the kinetic energy of water particles and presented a theoretical model to estimate the output parameters of a WEC having piezoelectric material patches. The electric power increases with various factors and can reach 55 W. Viet et al. [19]. designed a device that captures energy from waves in the ocean using a mass-spring system to convert wave motion to vibrations and a number of piezoelectric patches to turn the vibrations to electrical power. The results showed that the amount of power produced increases with higher ocean wave amplitudes and the device size and power decreases with longer ocean wave periods. The study concluded that the device could produce up to 103 W of power under specific conditions. Notle et al. [20] developed a theoretical model of a heavy type of WEC that converts vertical wave motion to rotational motion to harness substantial electrical energy. The vertical motion in the WEC system is due to the relative motion of ocean water particles. The two support methods that anchor the WEC to the ground

include moored systems and drogue anchored systems. Graves et al. [21] presented an innovative electromagnetic energy harvester having a pendulum as the inertial element, featuring a counterweight that efficiently captures low-frequency vibrations. This pioneering design allows for a reduction in the natural frequency of the pendulum with no change in its length, ensuring consistently better power output at lower frequencies compared to conventional pendulums of similar sizes. The pendulum-type energy harvester, with its integrated counterweight, demonstrates an impressive power generation of 0.997 W at 0.75 Hz. Furthermore, the system achieves an average normalized power output of 95.8 W/g^2 and an overall power density of 6.11 W/kg.

Chandrasekaran and Raghavi [22] have developed a wave energy converter using a buoy-type point absorber mounted on an offshore platform and converting wave energy into mechanical motion through a floating buoy and then electrical power using a generator. Tests show higher power output with increased wave heights, with a maximum mechanical power of about 127.08 W and mechanical efficiency of 23.47%. Li et al. [23] developed a prototype of an electromagnetic ocean wave energy harvester that employs a swing body device which can detect low-frequency wave energy and utilize it to drive an electromagnetic generator power module through transmission gears to deliver electric energy. Notably, as the wave height surpasses 0.6 m, the device achieves a maximum peak output voltage of 15.9 V, resulting in a power of up to 0.13 W with a peak power density of 0.2 mW/cm^3. Recently, there have been attempts by Wang et al. [24] to use wave energy to power sea environment monitoring sensor modules. These self-powered units improve the reliability and endurance of sea monitoring devices. Wang et al. proposed a new WEC device for marine applications made up of a buoy and an energy-generating unit. They conducted a simulation using hydrodynamic software and experimented on a 50 kg power-producing prototype, finding that it produced a maximum output peak voltage of 40 V under a wave height of 1.4 m and a wave time period of 4.5 s. Henriques et al. [25] developed two self-powered sensor buoys using the Oscillating-Water-Column (OWC) principle for long-term monitoring. The study focused on optimizing the buoy's hydrodynamic shape, turbine and generator selection, and control methods for the generator's electromagnetic torque. The research confirmed that OWC-based floating wave energy converters have the potential to power next-generation self-powered oceanographic buoys. Joe et al. [26] reduced the cost of Mooring-less Sensor Buoys with the use of a Wave Turbine System (WTS), which was implemented in full-scale application in the ocean environment, to deliver an average power of 1.61 W and a peak power of 37.68 W where the mean speed of the electric generator was 1120 rpm. Ding et al. [27] proposed a pendulum-type WEC as the sensor power source for an underwater glider, where experimentation revealed that the average output power of 150 mW at 0.8 Hz was enough for the sensor energy supply.

Chandrashekar et al. [28] proposed a spheroidal float hybrid generator with a Triboelectric Nanogenerator (TENG) and an electromagnetic generator (EMG) for the utilization of wave energy for useful electric power generation. The device generated maximum and average electrical voltage and current of 100 V or 2 μA and 20 V or 15 mA, respectively, where the output power was used to run position-tracking sensor nodes. Furthermore, a simple underwater communication system with a solar system was developed and evaluated in a pond. Hwangbo et al. [29] presented a self-powered marine monitoring system that produces renewable ocean energy from a device on the ocean surface and transmits the energy using an underwater energy collector and a battery controller. Zhang et al. [30] developed a self-powered triboelectric marine wave sensor manufactured with a round TENG and a hollow sphere buoy. The device can tune to the measurement of ocean waves in multiple directions, which eliminates the effect of water on the output of the system with sensors [31]. Lianga et al. [32] proposed a prototype MMR-based current collector

system for a WEC. This power take-off device, which transmits bi-directional shaft rotation to a unidirectional generator moving via a combination of two numbers of unidirectional bearings to a rack-and-pinion system. A shaft power converter containing a buoy with a 1.2 m long lever and an MMR-based PTO system is reported in this article. The peak output power is 205 W, while the average power is 21 W, with 63 W of average power harvested with the three phases [33,34].

Recent computational and experimental studies show a growing interest in inertia-amplified and motion-rectified wave energy converters (WECs). Chen [35] used high-fidelity CFD to analyze the inertial sea wave energy converter (ISWEC). They demonstrated nonlinear fluid-structure interaction (FSI) and improved energy capture through gyroscopic inertia. Similarly, Hung et al. [36] validated a mechanical motion rectifier (MMR) point absorber with both bench tests and simulations. Their results showed efficiency gains of about 10% with rectified PTO motion. Advancing this, Satpute et al. [37] introduced a two-way CFD-FEA framework for flexible WECs. They emphasized the importance of structural deformation and fatigue in realistic ocean conditions. Jia [38] presented a numerical analysis of an inertia-based WEC. Their findings confirmed that inertia amplification broadens the capture bandwidth under tuned conditions. More recently, Khedekar et al. [39] investigated active MMR (AMMR) configurations. They demonstrated better power smoothing and higher average capture efficiency compared to passive MMRs, further explored adaptive inertia tuning through internal water transfer [40]. Their dynamic inertia adjustments improved performance in irregular sea states. These studies highlight the need to combine CFD with detailed PTO modeling [41].

The current design differs by integrating a compact, manufacturable, passive MMR-based PTO with adaptive inertial tuning. It also employs full CFD-FSI validation at prototype scales. Unlike previous AMMR or gyroscopic studies, the proposed system focuses on manufacturability and robustness. It still allows for bandwidth broadening and peak-load reduction through simplified inertia control.

The literature survey indicates a pressing need to develop an efficient Wave Energy Converter (WEC) that can effectively harness wave motion for the generation of electrical power. Current designs face challenges in optimizing the utilization of wave kinetic energy due to inherent parasitic displacements of the waves. Additionally, there is a necessity to accommodate a broad range of wave heights, from very low to high, to maximize energy extraction. Existing Oscillating Water Column (OWC) and buoy-type WEC designs achieve a maximum energy conversion efficiency of only up to 32%. This paper introduces a novel WEC design that significantly advances the field. The proposed device includes a buoy, Mechanical Motion Rectifier (MMR), Motion Rectifier (MR), Energy Storage Element (ESE), and an electrical generator, all tailored to effectively utilize varying water wave heights for enhanced electrical power generation.

2. Construction and Working

The WEH arrangement involves the transformation of an oscillating wave force into useful electrical power that can be utilized for various purposes. The arrangement, depicted in Figure 1, comprises the use of the following components:

- Mechanical Motion Rectifier (MMR)
- Motion Regulator (MR)
- Energy Storage Element (ESE) (utilizing a torsional spring)
- Gearbox
- Electric generator (rotary type).

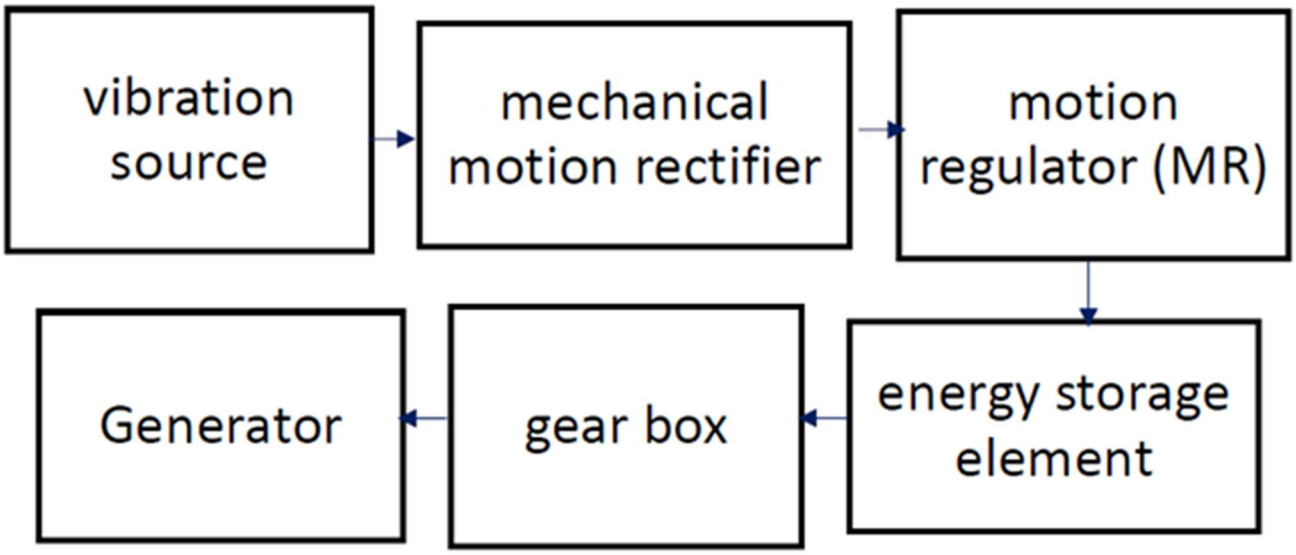

Figure 1. WEH block diagram.

The MMR converts the oscillations to unidirectional torque pulses. Further, the motion is then directed to the torsional spring through the MMR, which stores energy as strain energy. A minimum threshold amount of energy is accumulated in the spring due to the initial deflection. Additionally, torque pulses are transmitted from the MR to the spiral spring. The MR is designed in such a way that the torque pulses are transferred to the spiral spring, and it stores additional energy until the accumulated energy reaches a threshold limit. This limit is determined by the maximum deflection of the torsional spring. Thus, the MR ensures mechanical engagement when the torsional spring is deflected from its minimum to its maximum limit. As the spring accumulates energy up to the previously defined threshold value, the MR ensures that the MMR disengages from the spring. Consequently, the strain energy storage element, i.e., the spiral spring, becomes disengaged from the MMR as it receives energy up to the threshold limit.

As the MMR ensures that the torsional spring in ESE is disconnected from the source of vibration, it also ensures that the spring engages with the rotary electric generator. This allows the torsional spring to release its accumulated energy to the electric generator. Furthermore, as the strain energy in the spring decreases and the spring deflection becomes minimal, the MR ensures that the spring is mechanically disengaged from the electric generator. As a result, the strain energy storage component (i.e., the torsional spring) is deflected between its minimum and maximum limits and remains engaged with either the MR or the electric generator. The WEC is designed to convert wave oscillations into useful electric power and consists of mechanical motion rectification, motion regulation, an energy storage element in the form of a torsional spring, and an electric generator, where the block diagram is shown in Figure 2.

In Figure 3, the operation of the MMR is depicted. It transforms the back-and-forth wave motion into one-directional torque pulses. This mechanism involves mechanical levers, one-way bearings, and spherical joints. As shown in Figure 3, Lever 1 is anchored at point B, and the force is applied at the Float. Rod 1 moves back and forth concerning Lever 1 and is linked to Rod 2 using a spherical joint. Rod 2 is attached to Lever 2 through a sliding joint. Further, Lever 2 is fastened to the frame using a rotary joint with a one-way bearing. Lever 2 drives Shaft 1 through a rotary joint with another one-way bearing. This setup guarantees that the linear back-and-forth force applied at point B is turned into one-directional torque pulses at Shaft 1.

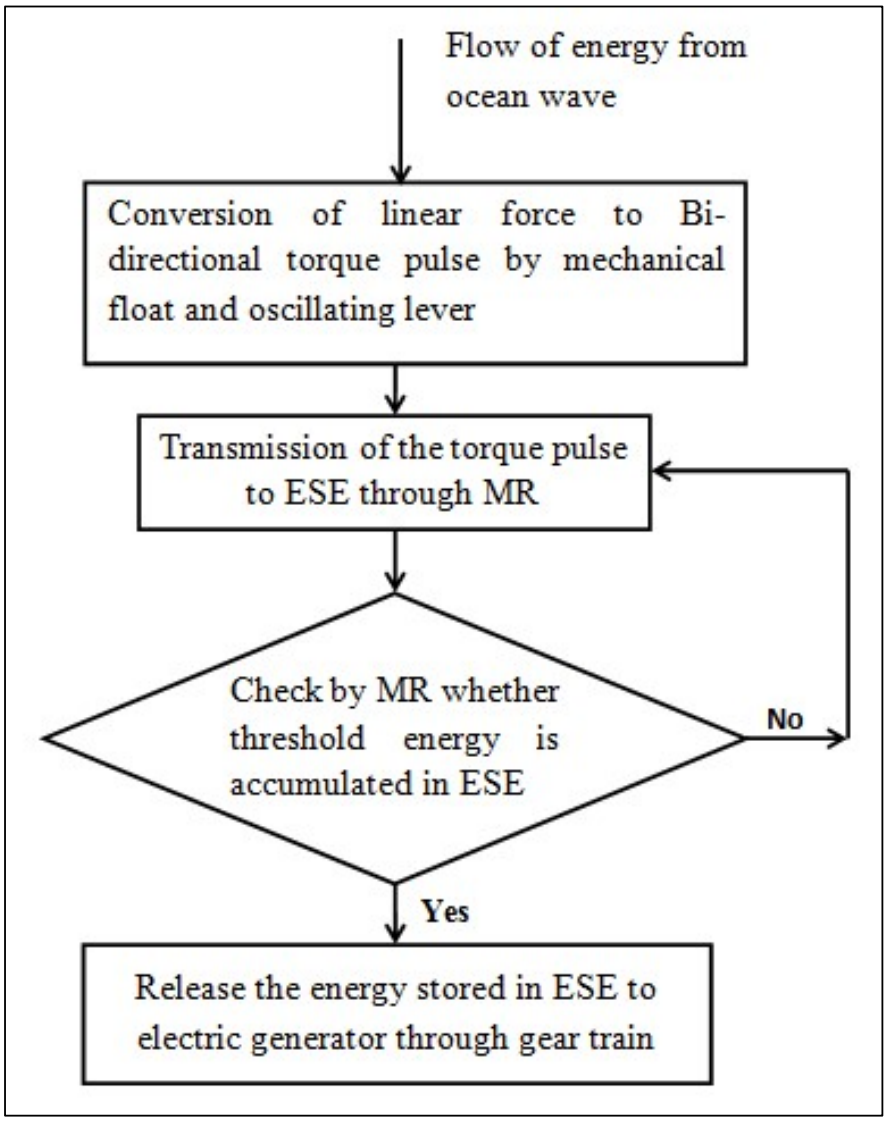

Figure 2. WEC working block diagram.

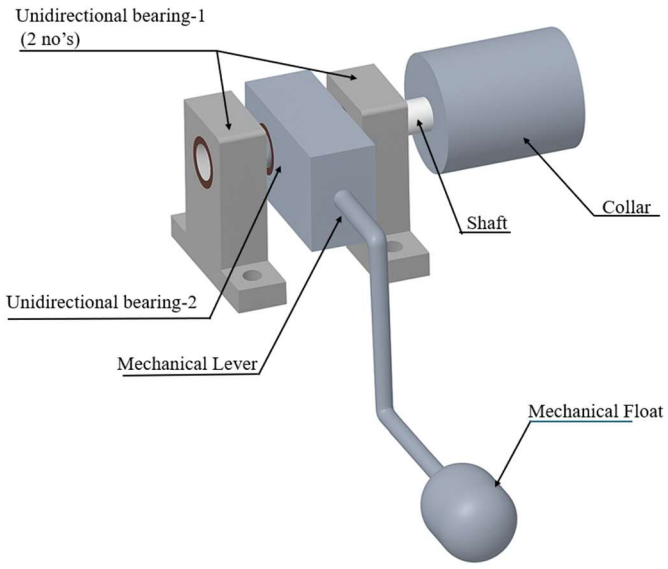

Figure 3. Working of the WEC Buoy.

3. Theoretical Modeling and Simulation

Mathematical modeling of the proposed wave energy harvester was used to determine its voltage and electrical power.

The proposed WEH operates in energy storage and energy release modes. The instantaneous torque at the spring as it is driven by the MMR in energy storage mode is given as:

$$T = Fl - K(\varnothing_{in} + \theta) - {G_r}^2 C_{el}\dot{\theta} \quad (1)$$

where:

F: Vertical force on the buoy due to wave motion (N)

l: Distance between the buoy's center of gravity and the rotational axes of the MMR (m)

K: ESE torsion spring stiffness (N-m/rad)

$\varnothing_{in}$: Initial deflection in the torsion spring (degree)

θ: Angular deflection of MMR and ESE (degree)

C_{el}*:* Electromagnetic rotary damping coefficient of the electrical generator (N-m-s/rad)

G_r*:* Gear ratio between ESE and the electric generator

Morris's equation is used to determine the vertical force due to the wave motion.

The wave vertical velocity is given as:

$$u_z = \frac{\pi H_w}{t}\left(\frac{\cosh k(D+z)}{\sinh(k*D)}\right)\cos(k - \omega t) \quad (2)$$

where:

H_w*:* Max wave height (m)

t: Time period of wave (s)

k: Wave number (2π/L) (m^{-1})

z: Wave depth (m)

D: Ocean depth (m).

The vertical force on the buoy is given as:

$$f_y = \frac{1}{2} C_d\ \rho\ A_z u_z^2\ m_f\ g \quad (3)$$

where

$C_{d:}$ Drag coefficient

ρ*:* Water density (kg/m^3)

A_z*:* Final projected area (m^2)

u_z *:* Acceleration in vertical direction (m/s^2)

m_f *:* mass of the fluid (kg).

Instantaneous energy stored in the ESE during the energy storage mode is given as:

$$E_{in} = K\left(\theta^2 - \varnothing_{in}^2\right) \quad (4)$$

It can be noted that the electric generator is connected to the ESE and is driven during both of the operating modes of the WEH. The governing differential equations for the WEH during the energy storage mode are given as:

$$I_{eq}\ddot{\theta} + {G_r}^2 C_{el}\dot{\theta}\ +\ K\theta = F_v l \quad (5)$$

where

I_{eq}*:* Equivalent rotary moment of inertia of the WEH in the energy storage mode ($kg \cdot m^2$).

The equivalent rotary moment of inertia of the WEH is further given as:

$$I_{e1} = I_1 + G^2 I_{em} \quad (6)$$

where

I_1: Rotary moment of inertia of the MMR, MR, and ESE ($kg \cdot m^2$)

I_{em}: Rotary moment of inertia of the electric generator ($kg \cdot m^2$).

The differential equation for the energy release mode, when the strain energy stored in the ESE drives the rotary electrical generator, is given as

$$I_{eq2}\ddot{\theta} + {G_r}^2 C_{em}\dot{\theta} = K\theta \quad (7)$$

where

I_{eq2}: The equivalent rotary moment of inertia of the WEH in the energy release mode ($kg \cdot m^2$).

The equivalent rotary moment of inertia of the WEH in the energy release is further given as:

$$I_{eq2} = I_2 + {G_r}^2 I_{em} \quad (8)$$

where

I_{eq2}: Rotary moment of inertia of MR and ESE (kg-m^2).

The voltage generated at the electric generator as measured across the load resistance is given as

$$V = \frac{\pi {D_{ar}}^2 NB\ R_l}{2(R_i + R_l)}\dot{\theta} \quad (9)$$

where

D_{ar}: Average copper coil diameter in the electric generator (m)

N: Number of turns in the generator armature coils

B: Magnetic flux density in the electric generator air gap (T)

R_l: Electric load resistance (Ω)

R_i: Internal resistance of the generator (Ω).

The electric power harvested by the generator is given as:

$$P = V^2 / R_l \quad (10)$$

During the numerical simulation, Equations (1)–(10) were solved in MATLAB–Simulink to calculate the voltage and power harvested by the energy harvester for the given wave motion. The Bagocki–Shmapine solver with a fixed time step of 0.01 s was used for the simulations.

4. Experimentation

The prototype was subjected to a test to determine the electrical power output in controlled wave conditions. The trials were conducted in a 1200 mm × 500 mm × 500 mm container equipped with a wave-producing arrangement. A DC motor of 400 W, driving between 20–600 rpm, was utilized to operate a scotch yoke mechanism. By rotation of the eccentric pin, the yoke transmitted a 60 mm harmonic stroke to the follower. This paddle, attached to a baffle plate, caused wave motion in the tank. The wave characteristics were mostly influenced by the frequency of the motor. The research tested wave heights of 50 mm, 60 mm, and 70 mm.

The experimental arrangement placed the buoy in the container of water, whereas the energy generation unit was mounted firmly outside the container. The buoy transmitted the wave energy to ESE through the MMR and MR, which further operated the rotary

electric generator. A load resistance of 12 Ω was used across the electric generator. The terminals of the generator and the voltage waveform armature resistance were measured with an oscilloscope (Make: Tektronix). Energy harvesting experiments using the prototype WEH were performed in two steps. Initially, the prototype WEH was operated with the buoy, MMR, MR, ESE, and the electric generator, as illustrated in Figures 3 and 4. Later, in the second arrangement, the WEH was operated with the buoy directly driving the electric generator. In the second arrangement, the MMR, MR, and ESE were not used and The WEH was operated using a conventional setup. The CAD model of the arrangement is shown in Figure 5, and the corresponding experimental test setup is shown in Figure 6.

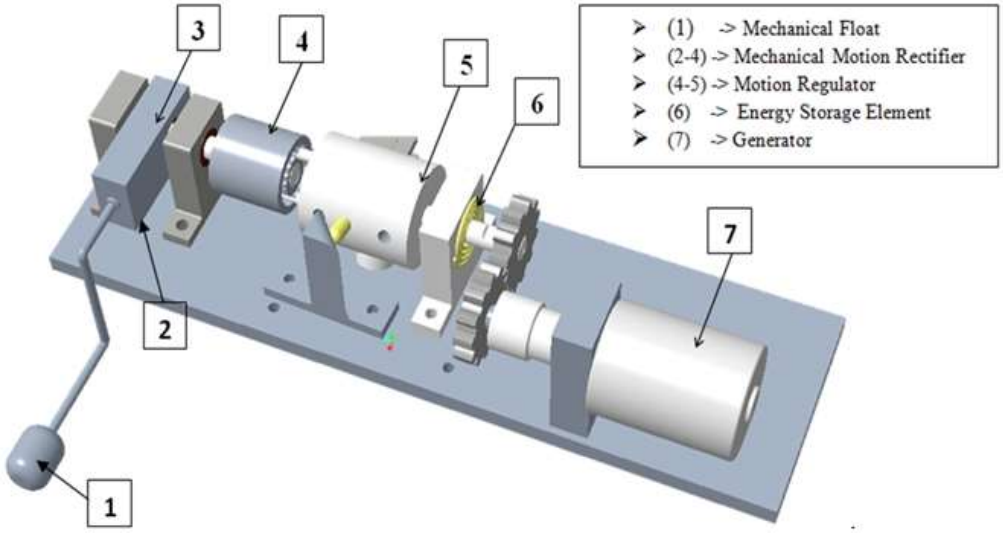

Figure 4. CAD model of WEH.

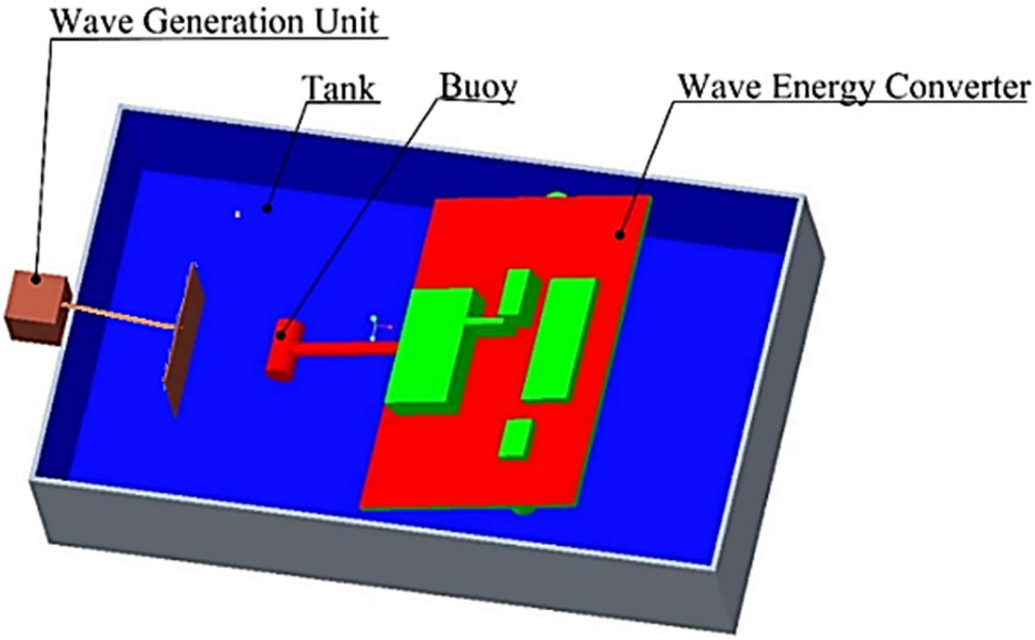

Figure 5. Experimental arrangement for energy harvesting in a container.

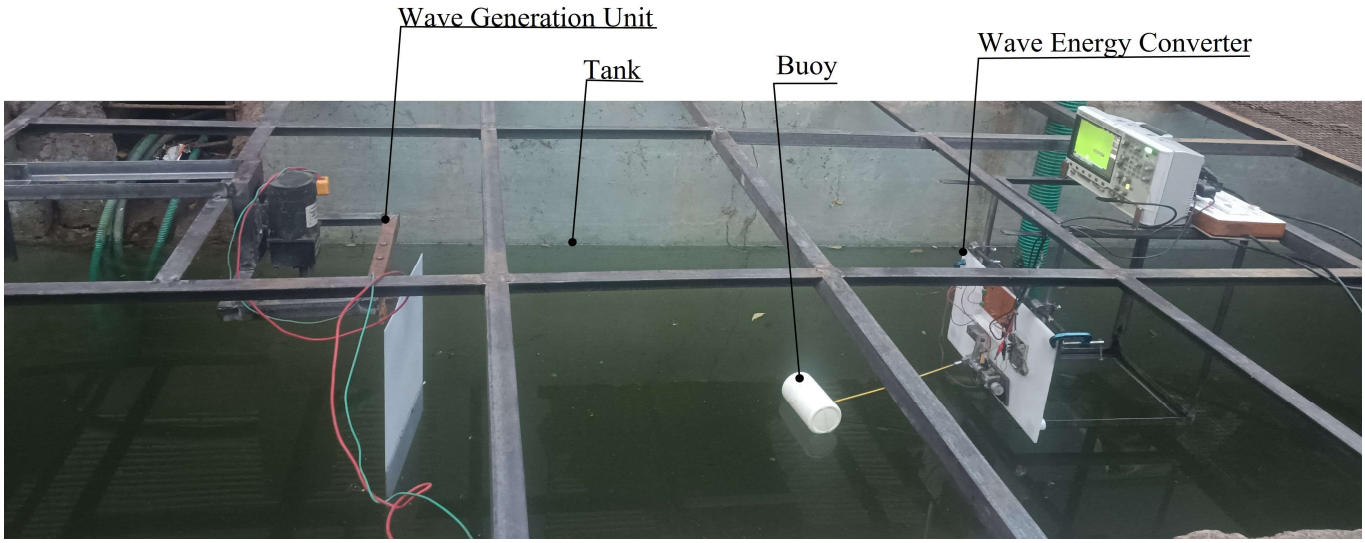

Figure 6. Experimental arrangement for energy harvesting in a tank.

5. Results and Discussion

Experimental and simulation studies are performed on the prototype to validate the mathematical model of the WEC. Numerical simulation is performed with the MATLAB model to determine the wave vertical force generated by the mechanical buoy. Simulation results for the vertical force on the mechanical buoy in the case of the wave height of 50 mm are shown in Figure 7.

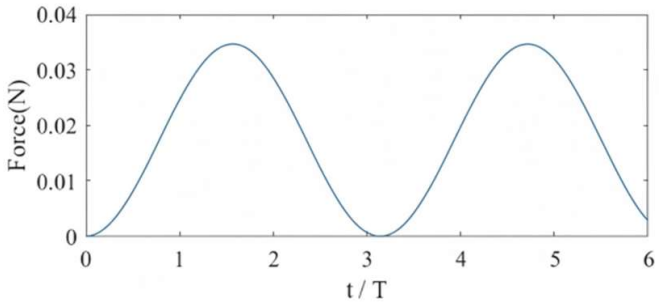

Figure 7. Vertical force for wave height of 50 mm.

It is noted that the prototype WEH operates in energy storage and release modes, where the electrical generator rotates slowly with MMR and MR during the energy storage mode. On the other hand, when the energy release mode is effective, the generator rotates at higher speed due to the release of the energy stored in the ESE. A MATLAB model was used to estimate the voltage generated for the energy storage and release modes. Figures 8 and 9 compare the theoretical analysis and experimental results for the voltage generated in the energy storage mode and energy release modes corresponding to 50 mm and 80 mm wave heights, where the wave time periods were 2.2 s and 1.7 s, respectively for.

The peak voltage for the energy storage mode was 20 mV and 32 mV, whereas that during the energy release mode was 6.7 V. It can be noted that the peak voltage during the energy storage mode varies with the wave height, since the generator is driven by the wave force directly through the buoy, MMR, MR, and ESE. However, during the energy release mode, the peak voltage does not depend on the wave height, since during this mode the ESE drives the electric generator. It can be noted from Figures 8 and 9 that the maximum difference between the simulation and experimental results for voltage was up to 8%, which validates the accuracy of the WEH MATLAB model.

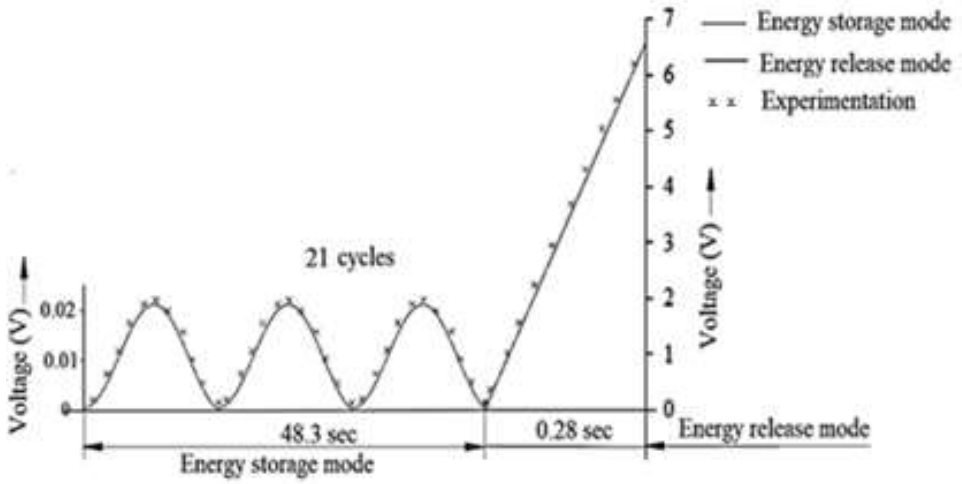

Figure 8. Voltage generated for wave height of 50 mm.

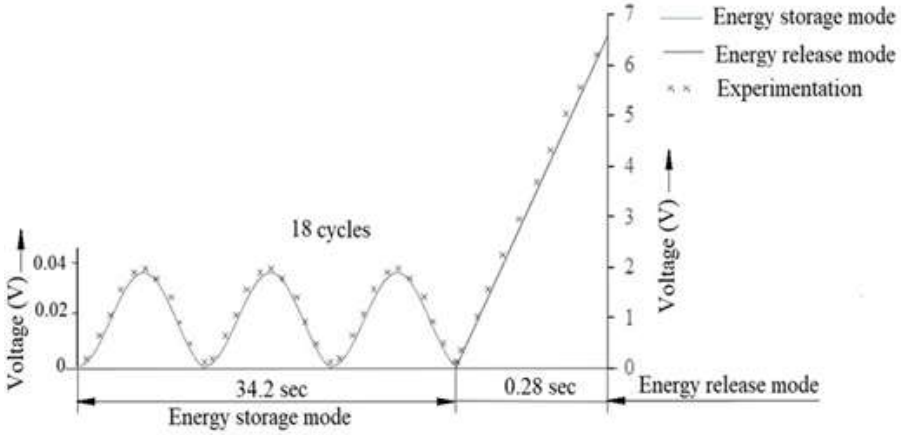

Figure 9. Voltage generated for a wave height of 80 mm.

Simulations were performed using the MATLAB model for an 80 mm wave height and a time period of 1.9 s to study the variation of the output electric power with the load resistance. The results shown in Figure 10 reveal that the prototype WEH will deliver a peak power of 3.6 W at a peak voltage of 6.45 V for a load resistance of 19.0 ℧.

From Figures 11 and 12, it is noted that the voltage and power generation significantly vary during the working of the WEH, and substantial power is harvested for energy release mode. The total energy harvested during a single cycle of the energy storage mode and energy release mode is given by Equation (11):

$$E_t = \frac{1}{R_l}\int V^2 dt \tag{11}$$

The average power generated by the Wave Energy Harvester (WEH) is determined by calculating the energy harvested during a single cycle, with the average power defined as *Average Power = Et/time duration of the single cycle*, considering both the energy storage and energy release modes. Simulations were conducted to analyze the variation in average electrical power across different wave heights, with the results illustrated in Figure 12. The findings indicate that average power increases with wave height, achieving a maximum of 4 W at a wave height of 100 mm. However, the peak power remains unchanged with varying wave heights, consistently measured at 4.09 W, where the peak power is calculated as *Peak Power* = V_{pk}^2/R_l, V_{pk} representing the peak voltage during the energy release mode.

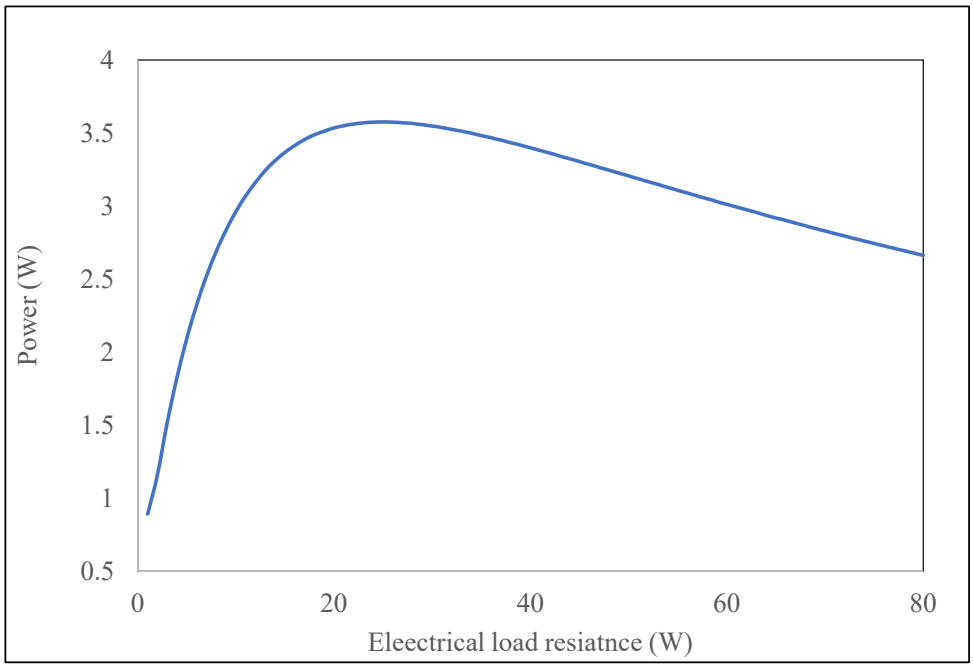

Figure 10. Variation of voltage and peak power with load resistance.

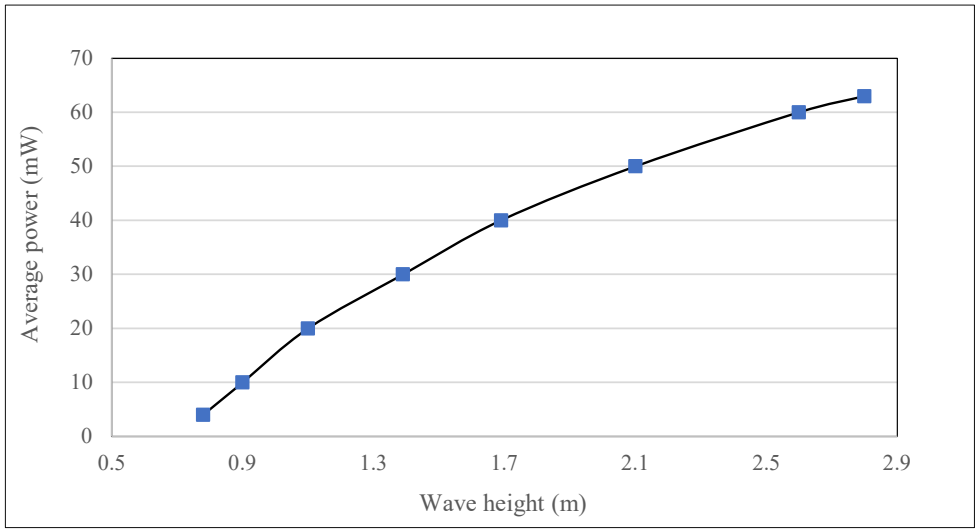

Figure 11. Variation of average power with wave height for prototype WEH (50–100 mm wave height).

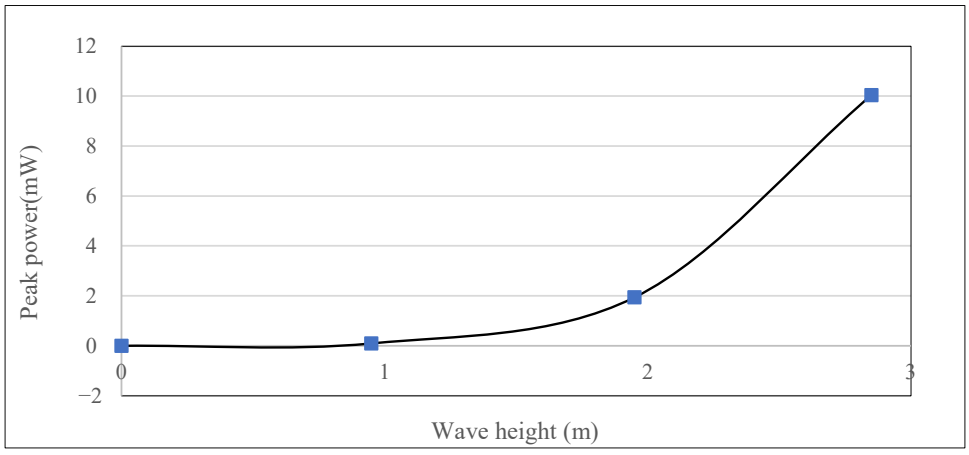

Figure 12. Peak power of the conventional WEH (50–100 mm wave height).

The conventional arrangement of the WEH is shown in Figure 3, with an oscillating buoy directly driving the electrical generator. MATLAB simulations were performed to determine the peak power harvested by the conventional WEH for different wave heights, and the results are given in Figure 12. During the simulation, the buoy and other dimensions of the WEH were kept identical to that of the earlier arrangement with the MMR and MR. Furthermore, simulations with the conventional arrangement were performed with an optimum electric load resistance of 12.0 Ω.

From Figure 13, it is noted that the peak power increases with wave height in the case of the conventional WEH. On the other hand, the peak power of the WEH with the MR and ESE remains constant, even if there are variations in the wave height and frequency. The WEH presented in this work will have the following advantages over the conventional design.

1. The voltage variation along a single cycle of energy storage and release for the conventional design and the WEH presented in this work is compared in Figures 13 and 14. It can be noted that peak voltage in the WEH presented in this work is significantly higher than that of the conventional design. Furthermore, it remains constant for changes in the wave height and frequency, which facilitates easy and efficient voltage conditioning for useful utilization of the harvested electric energy.
2. In order to use the harvested electric power for a useful application, the generated voltage needs to be higher than a threshold value. Figures 14 and 15 indicate that in the case of a utilization threshold voltage of 3.8 V, the conventional harvester will generate 22% useful electric energy, whereas the WEH presented in the work will generate 63% useful electric energy per cycle, comprising energy storage and release (energy = $\frac{1}{R_l}\int V^2 dt$).

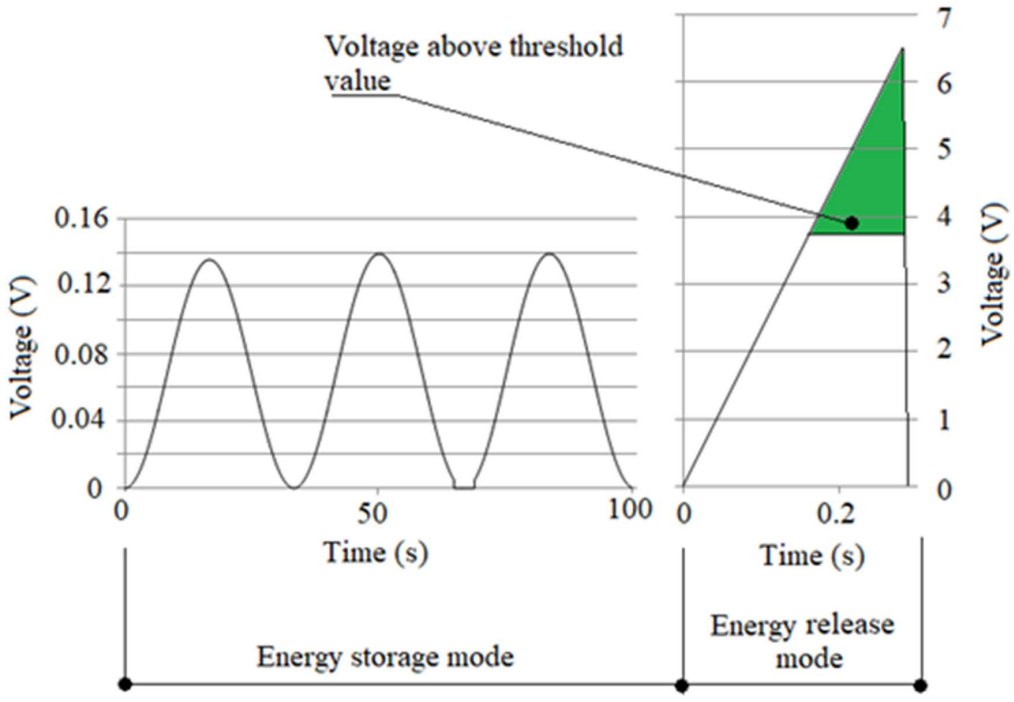

Figure 13. WEH voltage variation for wave height of 50 mm (time period = 2.1 s).

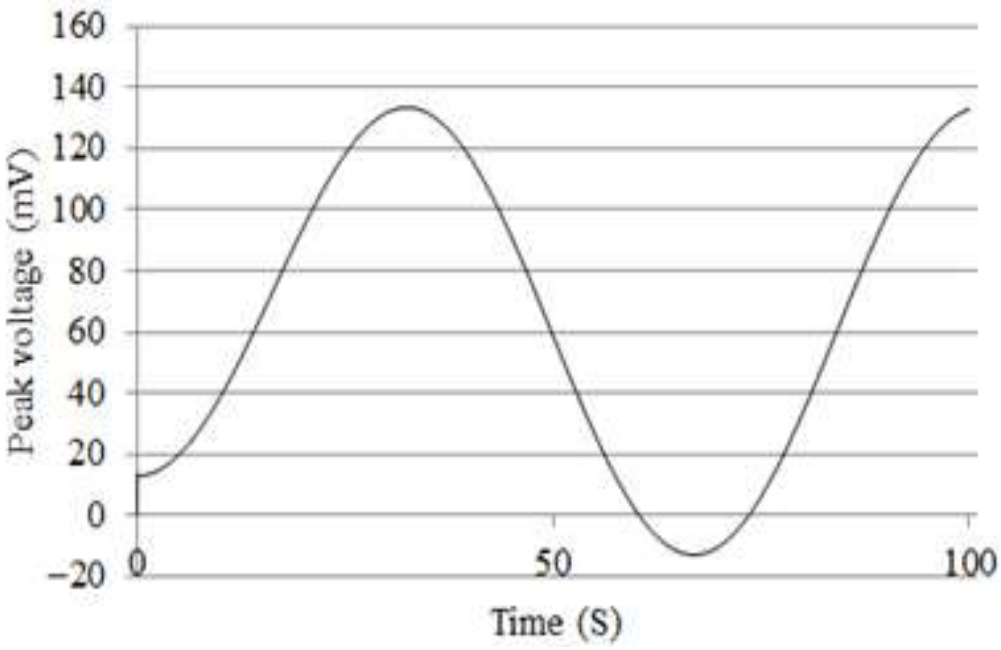

Figure 14. Conventional energy harvester voltage variation for wave height of 50 mm.

Figure 15. Experimental arrangement for energy harvesting along the seacoast.

Following the evaluation of the prototype using a laboratory test setup, additional experiments were conducted at sea to measure the average power output. The tests were performed at a location in Mumbai, Maharashtra, India. The experimental configuration for energy generation at the shore is depicted in Figure 15. In this setup, the buoy was placed in a container of water, while the energy generation unit was securely anchored to the ground. The buoy was subjected to wave conditions with heights ranging from 50 to 70 mm and periods of 5 to 7 s. The experiments took place in shallow seawater with a depth of 500 mm. Figure 15 also includes a photograph illustrating the prototype firmly supported with the buoy floating in the seawater. An oscilloscope, coupled with an uninterruptible power supply (UPS) equipped with batteries and an alternator, was used to record voltage waveforms during both the energy storage and energy release modes. The

shore-based experimentation yielded an average power output of 9.0 mW, with an energy storage duration of 137.0 s and 19 cycles required to complete a single energy storage mode.

After investigation of the experimental result and theoretical model, the design of the prototype WEH proposed to deliver a peak power of 68.06W and an average power 1.0 W. The arrangement, like that of the prototype, can be used in the actual size design with a cylindrical buoy used to transfer the wave force to the WEH. The torsional stiffness of the ESE is calculated based on the available torque from the wave vertical force due to wave height of 0.8–2.0 m and provides 8° to 16° of angular rotation of the buoy lever during each wave occurrence. Important specifications of the full-scale WEH are as follows:

1. Buoy size and dimensions: Cylindrical (1 m in length, 0.5 m in diameter).
2. Energy storage element torsional stiffness in the ESE: 120 N·m/rad.
3. The electric generator torsional damping coefficient used in the full-scale WEH: 0.05 N·m·s/rad.
4. Maximum angular rotation of the ESE during energy storage and release modes: 120°
5. Threshold energy stored in ESE: 125.6 J.
6. Load resistance connected to the electric generator: 400 Ω.
7. Rotating inertia of the MMR, ESE, and other components: 500 Kg·m^2.
8. Rotating inertia of the electric generator and equivalent inertia of the gears connected between the ESE and the electric generator: 600 Kg·m^2.

It can be noted that the gear ratio 'G' between the ESE and that of the electric generator is an important factor influencing power output. The lower value of the gear ratio results in lower damping torque; however, it also reduces power output since the harvested voltage is proportional to the gear ratio. On the other hand, the higher value of the gear ratio increases the damping torque to lower the generator's angular velocity, resulting in lower power output. Therefore, the optimization toolbox in MATLAB R 2022 is used to determine the above parameter for ensuring maximum power output. The details of the optimization are as follows:

1. Optimization method: Gradient descent
2. Maximum number of iterations: 1000
3. Functional tolerance: 1×10^{-6}
4. Lower and upper limits for 'G': 0.1 to 60

The optimization results indicated that the optimum gear ratio for the full scaled design was 46.8, which can be achieved by using two pairs of spur gears. Simulations were performed with the above-specified parameters to estimate the voltage, peak, and average power of the full-sized WEH. Simulation results for voltage variation in case of energy release mode are shown in Figure 16. Simulation results indicate that, for a wave height of 1.4 m, the full-sized design will take 3.0 s to complete one energy storage cycle. Variations of the average power for wave heights of 0.8–2.2 m are shown in Figure 17. The peak power harvested by the full-sized design during energy release mode will be 68.06 W and the average power will be 0.97 W.

Energy input during a single cycle of wave motion is calculated by using Equation (12)

$$E_{out} = \int_0^{\theta_{max}} F_v l d\theta \tag{12}$$

Electric energy generated by the rotary electric generator for a single cycle, comprising the energy storage mode and energy release mode, is given by Equation (13)

$$E_{in} = \frac{1}{R_l}\left[\int V^2 dt_{\,energystorage} + \int V^2 dt_{\,energyrelease}\right] \tag{13}$$

The overall efficiency of the full-scale Wave Energy Harvester (WEH) is calculated using the equations provided in Equations (12) and (13). Simulation results for the full-scale WEH reveal an overall efficiency of 76.2% when operating with a wave height of 1.6 m. Additionally, the total mass of the full-scale design is estimated to be 35.0 kg, encompassing various components such as the electric generator, energy storage element (ESE), Motion Rectifier (MR), buoy, gears, and shafts.

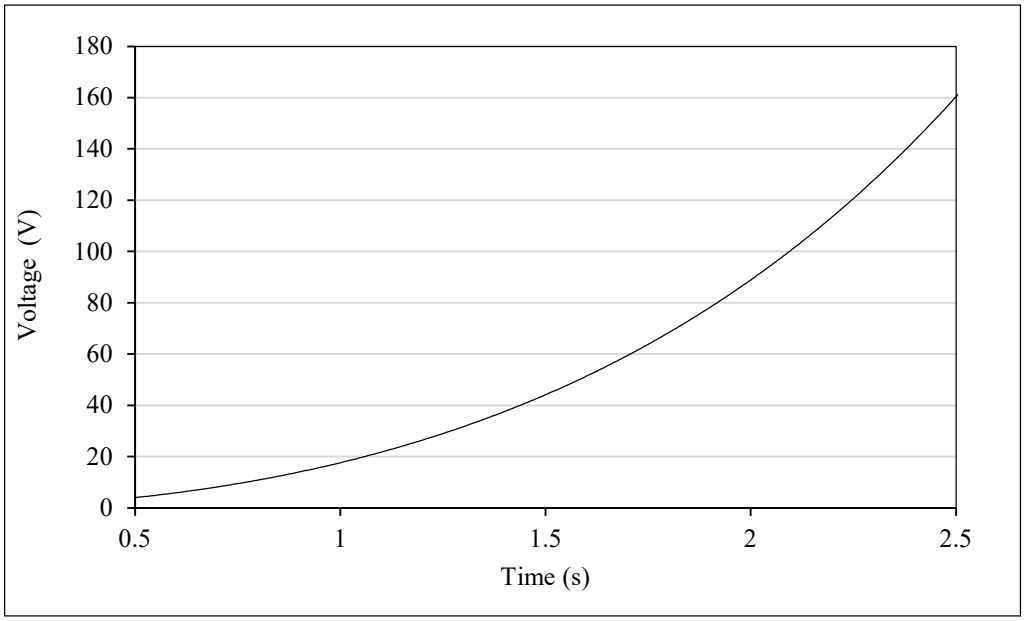

Figure 16. Voltage variation of full-scale WEH during energy release mode.

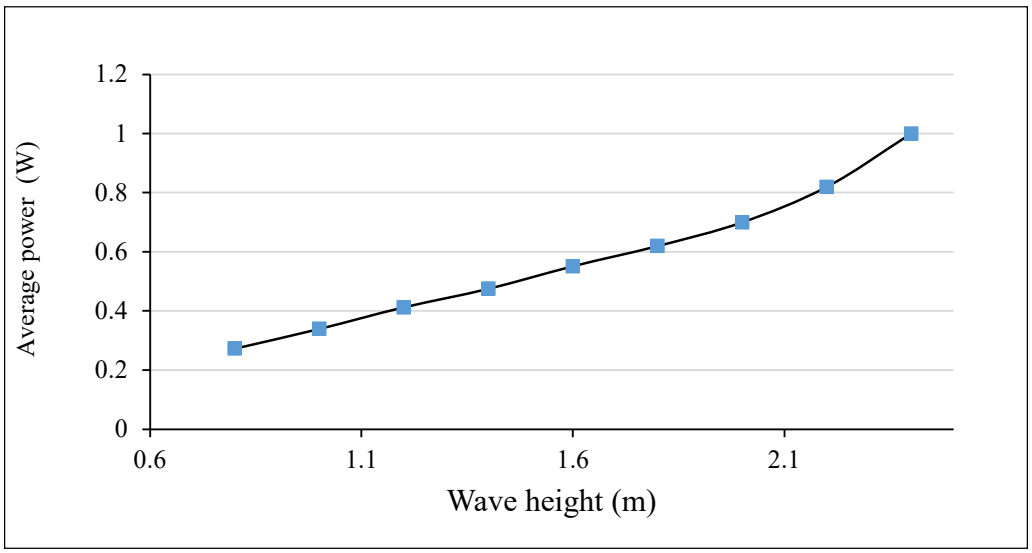

Figure 17. Variation of average power with wave height for full-scale WEH.

The prototype used in the present work has the spring directly driving the electric generator. This arrangement does not use gears between the torsional spring and electric generator, resulting in an effective gear ratio of 1.0. However, the full-scale design has an arrangement of gears between the spring and the generator with an optimum gear ratio of 46.8, which ensures maximum electric power from the generator. In the case of a size design, better electric power output ensures a higher energy harvesting efficiency of 76.2%. The increased energy harvesting efficiency of the full-scale design is attributed

to the effective damping coefficient of the electric generator, which is achieved due to the optimum value of the gear ratio between the spring and generator.

It can be noted that the torsional spring accumulates strain energy during the energy storage mode and releases the same during the energy release mode. Variations of the torque delivered by the torsional spring during the energy release mode are shown in Figure 18; variations in the voltage generated by the rotary electric generator are shown in Figures 8 and 9. It can be noted that there are significant variations in the torque and voltage during the time duration of energy release. An attempt has been made to propose an arrangement that will ensure smooth variation of the generated voltage during the energy release mode, which will further facilitate better voltage conditioning for effective utilization of the generated electric power.

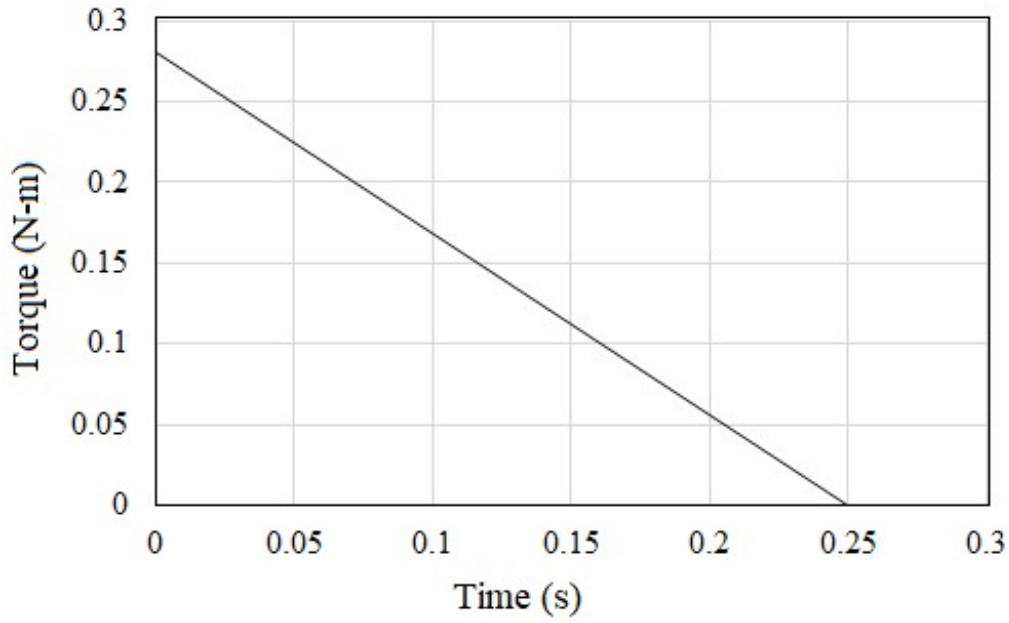

Figure 18. Variation of the spring torque during energy release mode.

The proposed arrangement has a quarter elliptical gear pinion driven by the torsional spring shown in Figure 19, which further drives a rack. The arrangement ensures that the effective engagement radius of the gear and at the start of the energy release mode, and the effective radius is higher at end of the energy release mode. There is an oscillating linear generator with the coils moving along the magnet-spacer array, such that the voltage is induced in the coils as it moves along the magnet-spacer array. The coils are connected to the rack, and the magnet-spacer array is pivoted at point 'X'. During the energy release mode, the torsional spring drives the gear, which makes the rack remove the copper coils in the linear generator relative to the magnet-spacer array. The magnet-spacer array is pivoted at the end to ensure that the arrangement can operate the linear generator. At the same time, the effective radius of the driving teeth changes from minimum to maximum during the energy release stroke. Variation in the effective radius ensures smooth release of the accumulated energy, leading to a uniform voltage waveform. Important parameters in the proposed arrangement are given below,

i. Ratio of the minimum radius of the gear to the maximum radius gear = 1/20
ii. Angle of the gear: 90 °
iii. Module of rack-gear arrangement: 2 mm
iv. Linear electrical damping coefficient of the linear generator: 0.5 N · s/m

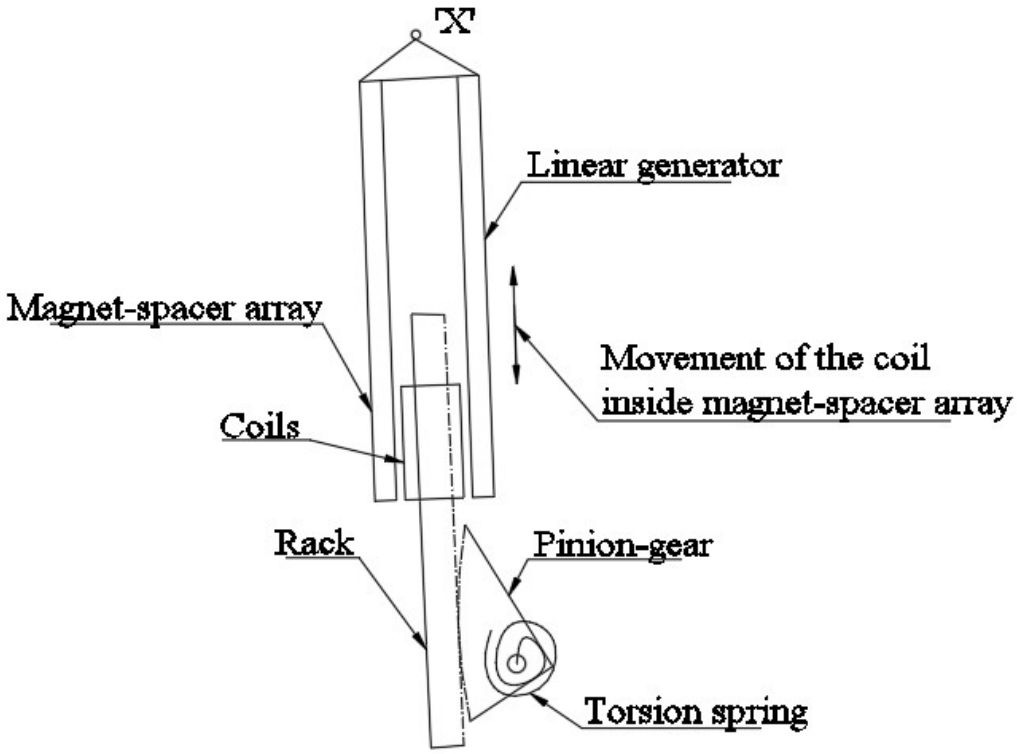

Figure 19. Arrangement with an elliptical gear-rack and oscillating linear generator.

The governing equation for the energy release mode with the above arrangement of the elliptical gear-rack and oscillating linear generator is given as

$$I_o\ddot{\theta} + K_t\theta + C_{lin}{r_t}^2\dot{\theta} = 0 \tag{14}$$

where

C_{lin}: Linear electrical damping coefficient of the linear generator
K_t: Torsional stiffness of the torsional spring
r_t: Instantaneous radius of the pinion gear.
The power delivered by the linear generator is given as

$$P_t = C_{lin}{r_t}^2\dot{\theta}^2 \tag{15}$$

Voltage at the linear generator output is given as

$$V(t) = \sqrt{P_t R_{load}} \tag{16}$$

where

R_{load} : load resistance at the electric generator.

Simulation results for the voltage delivered by the linear generator with the above arrangement of elliptical gear-rack and oscillating linear generator are given in Figure 20, which reveals that the proposed arrangement will ensure gradual release of the accumulated strain energy and result in a smoother voltage waveform during the energy release mode. Further, Figure 20 includes the voltage waveform with the earlier arrangement, which shows a linear increase in the voltage. The standard deviation for the voltage waveform with the use of the elliptical gear and linear generator is 1.71 V, whereas the standard deviation for the other arrangement is 2.44 V, which reveals the smooth variation of the voltage waveform in Figure 20.

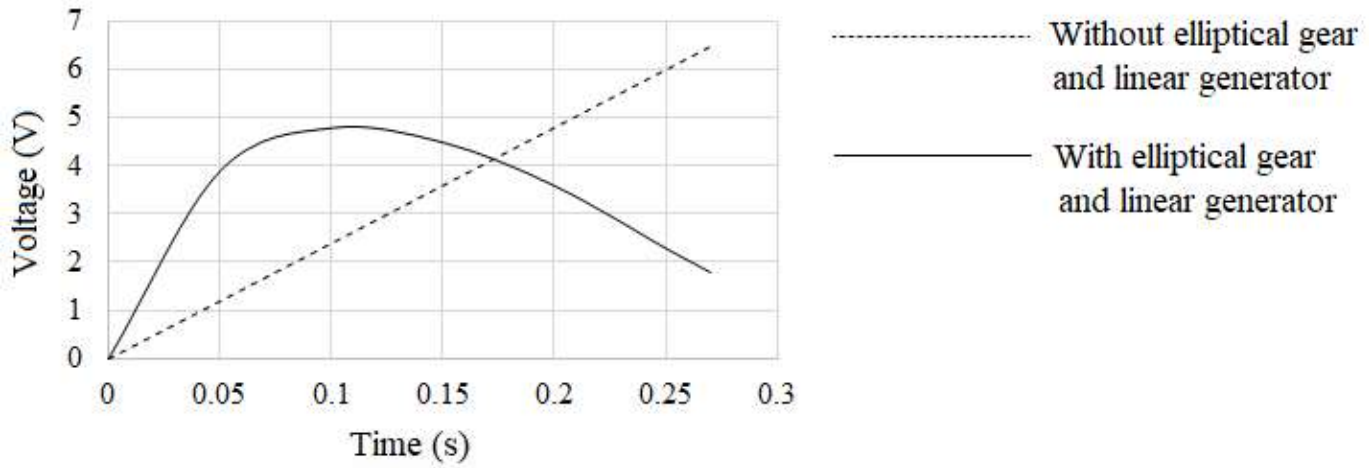

Figure 20. Variation of the generated voltage during energy release mode.

5.1. Simulation of Multimodal Operation with Additional Buoys

The proposed Wave Energy Converter (WEC) design utilizes three buoys in a multimodal arrangement to harness both vertical (heave) and horizontal (forward and backward) wave forces for electrical power generation.

The three forces acting on buoy used for WEC are:

Vertical Force: Arises from oscillating hydrostatic and dynamic pressures of passing wave crests and troughs, causing the buoy to move up and down (heave).

Horizontal Forward Force: Generated as a wave crest passes, pushing water toward the shore.

Horizontal Backward Force: Occurs as a wave trough passes, pulling water away from the shore toward the sea.

Similar to that of the wave forward force, the backward horizontal force acts when a wave trough passes. This results in pulling water into the ocean and creating horizontal backward force which acts toward the sea and away from the shore.

Both forward and backward forces occur in every wave cycle due to the circular kinematics of wave particles [42,43].

Although a WEC can be designed to utilize the wave vertical and horizontal forces, most of the reported literature work has focused on utilization of the wave vertical force. The reason for more focus on the vertical force is attributed to the following factors;

1. Simple design and mooring structure
2. Higher energy density in vertical forces than that of the horizontal forces.

5.2. Multimodal WEC Configuration

There is a possibility of using partially submerged buoys to harvest wave horizontal force for electric power generation [44–46]. An attempt is made in the present work to design a WEC capable of operating in a multimodal arrangement that can utilize wave vertical force, as well as the horizontal forward and backward forces for electric power generation.

The multimodal configuration, shown in Figures 21 and 22, employs three buoys connected to the input shaft of a Mechanical Motion Rectifier (MMR) (Table 1).

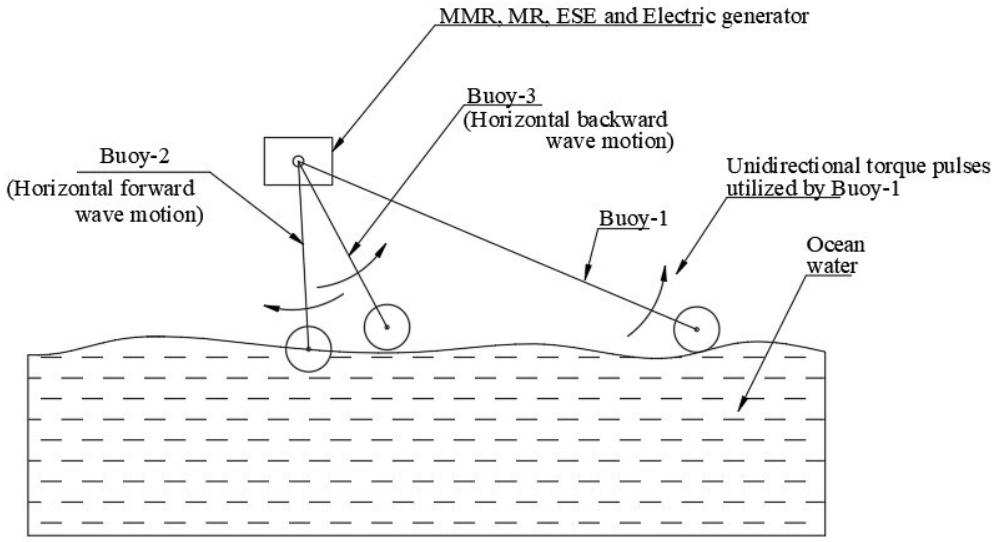

Figure 21. Arrangement with the additional buoy to utilize wave horizontal force.

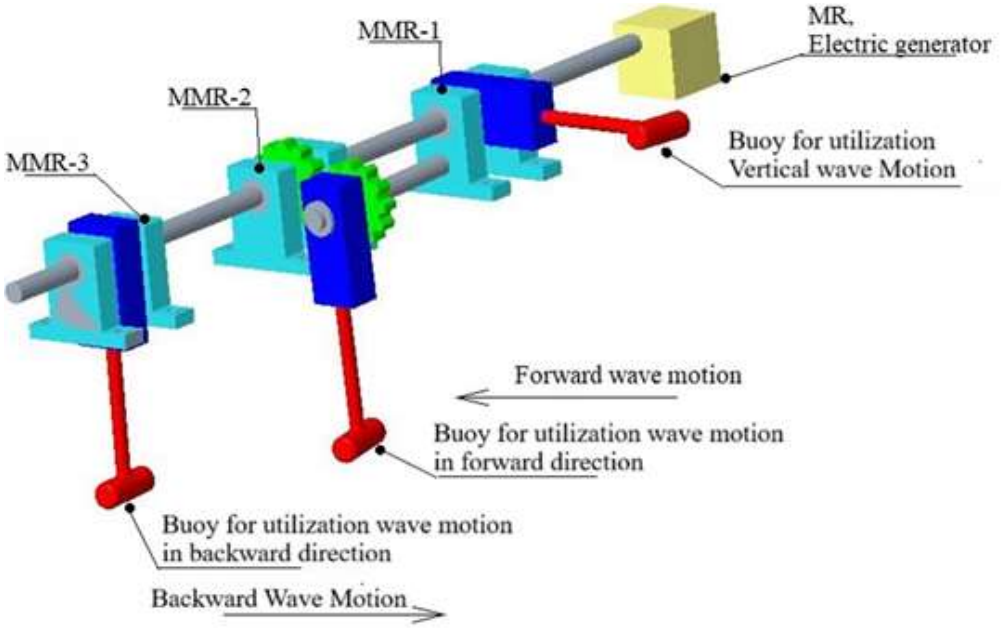

Figure 22. Incorporation of Buoy 2 and Buoy 3 in the MMR.

Table 1. Multimodal configuration of 3 Buoys.

Buoy	Position/Force Utilized	Purpose/Torque on MMR Shaft	Dimensions and Lever Length
Buoy 1	Afloat on the surface; utilizes Vertical Force.	Harnesses heave motion, applies anticlockwise torque to the MMR shaft.	Cylindrical (1.0 m length, 0.5 m diameter); 2.0 m lever length.
Buoy 2	Partially submerged, below the WEC structure; utilizes Horizontal Forward Force.	Initially applies clockwise torque but uses an additional support shaft and gear pair to ensure it applies anticlockwise torque to the MMR shaft, complementing Buoys 1 and 3.	1.5 m lever length; submerged part: 200 mm depth, 1.0 mm length.
Buoy 3	Partially submerged, below the WEC structure; utilizes Horizontal Backward Force.	Complements Buoy 1, applies anticlockwise torque to the MMR shaft.	1.5 m lever length; submerged part: 200 mm depth, 1.0 mm length.

Buoy 1 is connected to the WEC through a lever on one side away from the MMR input shaft, whereas Buoys 2 and 3 are located below the input shaft. The strategic use of the gear pair for Buoy 2 ensures that all three buoys apply a complementary anticlockwise torque on the MMR input shaft.

The length of levers connecting the Buoys (Buoys 1, 2, and 3) to the MMR input shaft should be long enough to provide sufficient angular displacement and torque. The angular displacement and torque applied at the MMR shaft will increase with increases to the length of the lever. However, a longer lever will also result in increased internal elastic deflection in the lever, which will reduce the effect of the torque and angular displacement transmitted to the MMR.

$$F_H = \frac{1}{2} C_d \rho D u_x l |u_x| + C_m \rho \pi \frac{D^2}{4} u_x l \quad (17)$$

where

C_d: Drag coefficient.
C_m: Inertia force coefficient
ρ: Water density (kg/m^3)
u_x: Water Velocity in the horizontal direction (m/s)
D: Diameter of the float (m)
l: Length of float (m).
The horizontal velocity of the wave is given by Equation (18)

$$u_x = \frac{\pi H}{T} \left(\frac{\sinh k(d+z)}{sinh(k*d)} \right) \sin(k - \omega t) \quad (18)$$

where

H: Maximum wave height (m)
T: Wave time period (s)
k: Wave number $2\pi/L$ (m^{-1})
z: Wave depth (m)
d: Ocean depth (m)
L: Wavelength (m).

Simulations incorporating the additional Buoy 2 and Buoy 3 alongside Buoy 1 have been conducted to leverage horizontal wave forces in addition to vertical forces. The results, presented in Figure 23, compare the average power outputs of two types of Wave Energy Converters (WECs). The Type-1 WEC employs a single buoy (Buoy 1) to harness vertical wave forces, whereas the Type-2 WEC integrates additional buoys (Buoy 2 and Buoy 3) to exploit horizontal wave forces. The data indicate that the inclusion of the additional buoys significantly enhances power output. Specifically, simulation results, as shown in Figure 23, demonstrate up to a 28% increase in average electrical power with the Type-2 WEC configuration.

The voltage variation during the energy release mode, as illustrated in Figures 9, 13 and 16, demonstrates fluctuations from zero to the maximum value. To optimize the utilization of harvested electrical power, it is preferable to achieve a more constant voltage output. Consequently, investigations have been conducted to incorporate non-circular elliptical gears in the power transmission system between the energy storage element (ESE) and the electric generator. This modification aims to provide a more stable voltage output, enhancing the overall efficiency of the power generation process.

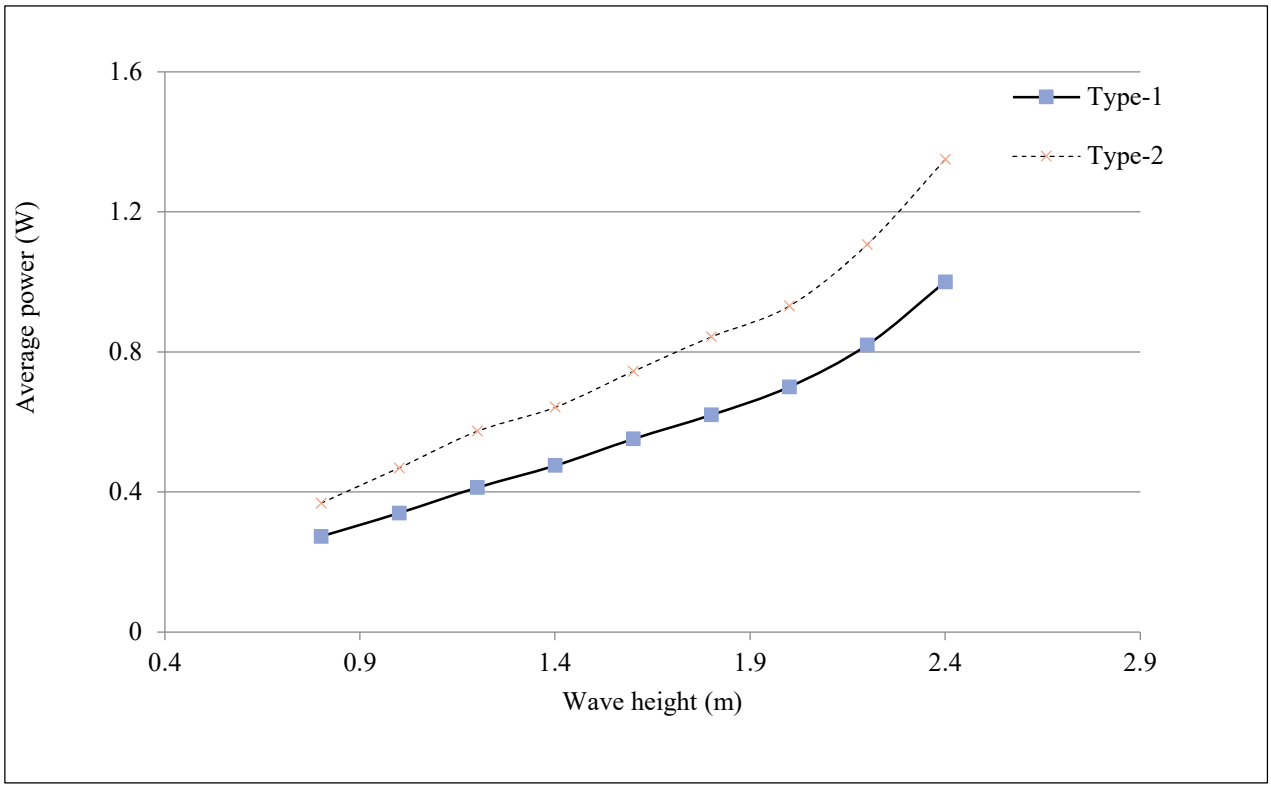

Figure 23. Average power harvested by WEC with the additional.

6. Conclusions

The presented work introduces a novel method for efficiently harvesting energy from ocean waves. The system, comprising a Mechanical Motion Rectifier (MMR), Motion Rectifier (MR), Energy Storage Element (ESE), and an electric generator, achieves an energy harvesting efficiency of 47.2% and demonstrates an improved voltage waveform for better utilization of the harvested electrical energy. The design is characterized by its simplicity and the use of cost-effective components in its assembly. Experimental tests and numerical simulations have shown that the prototype energy harvester can generate a peak voltage of 6.7 V and an average power of 8.5 mW. For the full-scale application of the proposed Wave Energy Converter (WEC), a peak power of 68.04 W and an average power ranging from 0.25 to 1.00 W can be achieved for wave heights between 0.8 and 2.2 m. Additionally, numerical simulations have been conducted to explore the use of elliptical gears in power transmission and the incorporation of additional buoys to harness horizontal wave forces, aiming to further enhance the WEC's output power. Seawater corrosion presents significant challenges to the durability of wave energy converters (WECs) in various marine environments. To address these challenges, protective strategies such as coatings, composites, and cathodic protection are essential. The use of advanced alloys and specialized composites enhances the resistance of motors and mechanical subsystems to corrosion. Although the current results are primarily based on simulations, future research will concentrate on prototype testing, scalability, reliability, and the trade-offs between cost and complexity.

Author Contributions: Conceptualization, G.K. and N.S.; methodology, G.K. and N.S.; software, G.K. and N.S.; validation, T.I.E., N.S. and A.P.K.; formal analysis, G.K. and N.S.; investigation, G.K. and A.S.; resources, N.S. and A.P.K.; data curation, G.K.; writing—original draft preparation, G.K. and N.S.; writing—review and editing, N.S., A.P.K., T.I.E. and A.S.; visualization, T.I.E. and A.S.; supervision, A.P.K. and A.S.; project administration, T.I.E. and N.S. All authors have read and agreed to the published version of the manuscript.

Funding: This work is not supported fully or partially by any funding organization or agency.

Institutional Review Board Statement: Not applicable.

Informed Consent Statement: Not applicable.

Data Availability Statement: The author confirms that the data supporting the findings of this study are available within the article. Any other data, if necessary, could be available by corresponding author on reasonable request.

Conflicts of Interest: The authors declare that there are no conflicts of interest regarding the publication of this paper.

List of Abbreviations

Symbol	Definition
WEC	Wave Energy Converter
PTO	Power Take-Off
LS-WEC	Linear Sliding Wave Energy Converter
eSpring	Electromagnetic Spring
RMS	Root Mean Square
Ka	Wavenumber
MFCC	Mel-Frequency Cepstral Coefficients
HMM	Hidden Markov Models
FMEA	Failure Mode and Effects Analysis
MPPT	Maximum Power Point Tracking
VQ	Vector Quantization
VIBR	Vibrational
RF	Radio Frequency
CMOS	Complementary Metal-Oxide-Semiconductor
LDDE	Low-Drop-Diode Equivalent
DC-DC	Direct Current to Direct Current
OOK	On-Off Keying
IC	Integrated Circuit
PZT	Lead Zirconate Titanate
TDMA	Time Division Multiple Access
FDMA	Frequency Division Multiple Access
LDO	Low Dropout Regulator
PWM	Pulse Width Modulation
BPSK	Binary Phase Shift Keying
MEMS	Micro-Electro-Mechanical Systems
SAW	Surface Acoustic Wave
PEH	Piezoelectric Energy Harvester

References

1. Liu, Z.; Xu, C.; Kim, K.; Choi, J.; Hyun, B.-S. An integrated numerical model for the chamber-turbine system of an oscillating water column wave energy converter. *Renew. Sustain. Energy Rev.* **2021**, *149*, 111350. [CrossRef]
2. Arena, F.; Laface, V.; Malara, G.; Meduri, S.; Pedroncini, A. Response Statistics of U-Oscillating Water Column Energy Harvesters Exposed to Extreme Storms: Application to the Case Study of Roccella Jonica (Italy). *ASME J. Risk Uncertain. Part B* **2021**, *7*, 010903. [CrossRef]
3. Setoguchi, T.; Takao, M. Current Status of Self-Rectifying Air Turbines for Wave Energy Conversion. *Energy Convers. Manag.* **2006**, *47*, 2382–2396. [CrossRef]
4. Takao, M.; Setoguchi, T. Air Turbines for Wave Energy Conversion. *Int. J. Rotating Mach.* **2012**, *2012*, 717398. [CrossRef]
5. Setoguchi, T.; Kaneko, K.; Maeda, H.; Kim, T.W.; Inoue, M. Impulse Turbine with Self-Pitch-Controlled Guide Vanes for Wave Power Conversion: Performance of Mono-Vane Type. *Int. J. Offshore Polar Eng.* **1993**, *3*, 73–78.

6. Moretti, G.; Papini, G.P.R.; Righi, M.; Forehand, D.; Ingram, D.; Vertechy, R.; Fontana, M. Resonant wave energy harvester based on dielectric elastomer generator. *Smart Mater. Struct.* **2018**, *27*, 035015. [CrossRef]
7. Kazemi, S.; Nili-Ahmadabadi, M.; Tavakoli, M.R.; Tikani, R. Energy harvesting from longitudinal and transverse motions of sea waves particles using a new waterproof piezoelectric waves energy harvester. *Renew. Energy* **2021**, *179*, 528–536. [CrossRef]
8. Karayaka, H.B.; Mahlke, H.; Bogucki, D.; Mehrubeoglu, M. A rotational wave energy conversion system development and validation with real ocean wave data. In Proceedings of the 2011 IEEE Power and Energy Society General Meeting, Detroit, MI, USA, 24–28 July 2011; pp. 5–11. [CrossRef]
9. Bou-Mosleh, C.; Rahme, P.; Beaino, P.; Mattar, R.; Nassif, E.A. Contribution to clean energy production using a novel wave energy converter: Renewable energy. In Proceedings of the 2014 International Conference on Renewable Energies for Developing Countries (REDEC), Beirut, Lebanon, 26–27 November 2014; pp. 108–111. [CrossRef]
10. Zanuttigh, B.; Angelelli, E. Experimental investigation of floating wave energy converters for coastal protection purpose. *Coast. Eng.* **2013**, *80*, 148–159. [CrossRef]
11. Akib, T.B.A.; Iqbal, I.; Mehedi, F. Numerical design and analysis of ocean wave energy generator. In Proceedings of the 2019 International Conference on Energy and Power Engineering (ICEPE), Dhaka, Bangladesh, 14–16 March 2019; pp. 31–34. [CrossRef]
12. Velichkova, R.; Stankov, P.; Simova, I.; Markov, D.; Angelova, R.A.; Pushkarov, M.; Denev, I. Integrated System for Wave Energy Harvesting. In Proceedings of the 2021 6th International Symposium on Environment-Friendly Energies and Applications (EFEA), Sofia, Bulgaria, 24–26 March 2021; pp. 2020–2023. [CrossRef]
13. Chen, H.M.; DelBalzo, D.R. Linear sliding wave energy converter. In Proceedings of the MTS/IEEE OCEANS 2015, Genova, Italy, 18–21 May 2015; pp. 1–6. [CrossRef]
14. Chen, H.M.; DelBalzo, D.R. Electromagnetic Spring for Sliding Wave Energy Converter. In Proceedings of the MTS/IEEE OCEANS 2015, Washington, DC, USA, 19–22 October 2015; pp. 1–5. [CrossRef]
15. Hossain, J. Energy Conversion System Using. In Proceedings of the 2016 4th International Conference on the Development in the in Renewable Energy Technology (ICDRET), Dhaka, Bangladesh, 7–9 January 2016; Volume 23, pp. 3–8.
16. Falnes, J.; Kurniawan, A. Fundamental formulae for wave-energy conversion. *R. Soc. Open Sci.* **2015**, *2*, 140305. [CrossRef] [PubMed]
17. Na, Y.-M.; Lee, H.-S.; Park, J.-K. A study on piezoelectric energy harvester using kinetic energy of ocean. *J. Mech. Sci. Technol.* **2018**, *32*, 4747–4755. [CrossRef]
18. Xie, X.D.; Wang, Q.; Wu, N. Potential of a Piezoelectric Energy Harvester from Sea Waves. *J. Sound Vib.* **2014**, *333*, 1421–1429. [CrossRef]
19. Viet, N.V.; Xie, X.D.; Liew, K.M.; Banthia, N.; Wang, Q. Energy Harvesting from Ocean Waves by a Floating Energy Harvester. *Energy* **2016**, *112*, 1219–1226. [CrossRef]
20. Nolte, J.D.; Ertekin, R.C. Wave power calculations for a wave energy conversion device connected to a drogue. *J. Renew. Sustain. Energy* **2014**, *6*, 013117. [CrossRef]
21. Graves, J.; Kuang, Y.; Zhu, M. Counterweight-pendulum energy harvester with reduced resonance frequency for unmanned surface vehicles. *Sensors Actuators A Phys.* **2021**, *321*, 112577. [CrossRef]
22. Chandrasekaran, S.; Raghavi, B. Design, Development and Experimentation of Deep Ocean Wave Energy Converter System. *Energy Procedia* **2015**, *79*, 634–640. [CrossRef]
23. Li, Y.; Guo, Q.; Huang, M.; Ma, X.; Chen, Z.; Liu, H.; Sun, L. Study of an electromagnetic ocean wave energy harvester driven by an efficient swing body toward the self-powered ocean buoy application. *IEEE Access* **2019**, *7*, 129758–129769. [CrossRef]
24. Wang, H.; Wu, W.; Zhu, L.; Koutroulis, E.; Lu, K.; Blaabjerg, F. Design and Experiment of a New Wave Power Conversion Device for Self-Powered Sensor Buoy. In Proceedings of the IECON 2021—47th Annual Conference of the IEEE Industrial Electronics Society, Toronto, ON, Canada, 13–16 October 2021.
25. Henriques, J.; Portillo, J.; Gato, L.; Gomes, R.; Ferreira, D.; Falcão, A. Design of oscillating-water-column wave energy converters with an application to self-powered sensor buoys. *Energy* **2016**, *112*, 852–867. [CrossRef]
26. Joe, H.; Roh, H.; Cho, H.; Yu, S.-C. Development of a flap-type mooring-less wave energy harvesting system for sensor buoy. *Energy* **2017**, *133*, 851–863. [CrossRef]
27. Ding, W.; Song, B.; Mao, Z.; Wang, K. Experimental investigation on an ocean kinetic energy harvester for underwater gliders. In Proceedings of the 2015 IEEE Energy Conversion Congress and Exposition (ECCE), Montreal, QC, Canada, 20–24 September 2015; Volume 782, pp. 1035–1038. [CrossRef]
28. Chandrasekhar, A.; Vivekananthan, V.; Kim, S.-J. Packed Spheroidal Hybrid Generator for Water Wave Energy Harvesting and Self-Powered Position Tracking. *Nano Energy* **2019**, *69*, 104439. [CrossRef]
29. Hwangbo, S.; Jeon, J.; Park, S. Self-Powered Wireless Ocean Monitoring Systems. In Proceedings of the 6th International Conference on Sensor Technologies and Applications (SENSORCOMM), Rome, Italy, 19–24 August 2012; pp. 334–337.
30. Zhang, C.; Liu, L.; Zhou, L.; Yin, X.; Wei, X.; Hu, Y.; Liu, Y.; Chen, S.; Wang, J.; Wang, Z.L. Self-Powered Sensor for Quantifying Ocean Surface Water Waves Based on Triboelectric Nanogenerator. *ACS Nano* **2020**, *14*, 7092–7100. [CrossRef]

31. Xie, Q.; Zhang, T.; Pan, Y.; Zhang, Z.; Yuan, Y.; Liu, Y. A novel oscillating buoy wave energy harvester based on a spatial double X-shaped mechanism for self-powered sensors in sea-crossing bridges. *Energy Convers. Manag.* **2020**, *204*, 112286. [CrossRef]
32. Liang, C.; Ai, J.; Zuo, L. Design, fabrication, simulation and testing of an ocean wave energy converter with mechanical motion rectifier. *Ocean Eng.* **2017**, *136*, 190–200. [CrossRef]
33. Yang, Y.; Chen, P.; Liu, Q. A wave energy harvester based on coaxial mechanical motion rectifier and variable inertia flywheel. *Appl. Energy* **2021**, *302*, 117528. [CrossRef]
34. Boldea, I. *Variable Speed Generators*; CRC Press: Boca Raton, FL, USA; Taylor & Francis: London, UK, 2016; p. 600. [CrossRef]
35. Chen, B. Wave Energy Converter with Mechanical Motion Rectifier Power Take-Off System. Master's Thesis, Virginia Tech, Blacksburg, VA, USA, 2021. Available online: https://vtechworks.lib.vt.edu/handle/10919/103994 (accessed on 7 August 2024).
36. Huang, C.; Shao, Y.; He, G.; Lin, Z. A CFD–FEA coupled method for fluid–structure interaction of flexible wave energy converters. *Phys. Fluids* **2023**, *35*, 077101. [CrossRef]
37. Satpute, N.; Jugulkar, L.; Jabade, S.; Korwar, G.; Arawade, S. Design and analysis of motion and energy regulating vibration harvester. *Proc. Inst. Mech. Eng. Part C J. Mech. Eng. Sci.* **2022**, *236*, 1391–1405. [CrossRef]
38. Jia, H. Modeling and analysis of inertia wave energy converters. *Energies* **2023**, *16*, 5376. [CrossRef]
39. Khedkar, P.H.; Sannasiraj, S.A.; Sundar, V. Numerical investigation of inertial sea wave energy converter (ISWEC) using CFD. *Ocean. Eng.* **2021**, *239*, 109819. [CrossRef]
40. Maria-Arenas, A.; Garrido, A.J.; Garrido, I.; Garrido, M. Adaptive inertia tuning in wave energy converters via internal fluid transfer. *J. Mar. Sci. Eng.* **2024**, *12*, 245. [CrossRef]
41. Yang, X.; Li, Z.; Zhou, M. Design and optimisation of active mechanical motion rectifier for wave energy conversion. *Renew. Energy* **2024**, *224*, 1205–1218. [CrossRef]
42. Semeraro, F.; Zitti, G.; Arena, F. Experimental and Numerical Investigation of a Heaving Buoy Wave Energy Converter. *Energies* **2015**, *8*, 13443–13460. [CrossRef]
43. Folley, M.; Whittaker, T.J.T.; van't Hoff, J. The control of wave energy converters using active bipolar damping. *Proc. Inst. Mech. Eng. Part A J. Power Energy* **2009**, *223*, 479–487. [CrossRef]
44. Xu, S.; Xu, J.; Li, W.; Zhang, Y. Numerical Simulation and Analysis of a Point Absorber Wave Energy Converter with Different Power Take-off Systems. *Renew. Energy* **2016**, *96*, 479–489. [CrossRef]
45. Zhu, G.; Shahroozi, Z.; Zheng, S.; Göteman, M.; Engström, J.; Greaves, D. Experimental study of interactions between focused waves and a point absorber wave energy converter. *Ocean Eng.* **2023**, *287*, 115815. [CrossRef]
46. Ropero-Giralda, P.; Crespo, A.J.; Tagliafierro, B.; Altomare, C.; Domínguez, J.M.; Gómez-Gesteira, M.; Viccione, G. Efficiency and survivability analysis of a point-absorber wave energy converter using DualSPHysics. *Renew. Energy* **2020**, *162*, 1763–1776. [CrossRef]